

Utilizing Sentinel-2 Remote Sensing for Water Quality Monitoring in Deran Lake, Bosnia and Herzegovina

Anja Batina¹, Ante Šiljeg², Gloria Pedić³, Marija Parać⁴

¹ University of Zadar, Center for geospatial technologies, Trg kneza Višeslava 9, 23000 Zadar, Croatia - abatina@unizd.hr

² University of Zadar, Department of Geography, Trg kneza Višeslava 9, 23000 Zadar, Croatia - asiljeg@unizd.hr

³ University of Zadar, Center for geospatial technologies, Trg kneza Višeslava 9, 23000 Zadar, Croatia - gpedic@unizd.hr

⁴ Ruđer Bošković Institute, Division for Marine and Environmental Research, Laboratory for physical chemistry of traces, Bijenička cesta 54, 10000 Zagreb, Croatia - mparac@irb.hr

Keywords: Atmospheric correction, Case-2 Regional Coast Colour, Pixel window size, QGIS, Spatial averaging, SNAP.

Abstract

This study evaluates the effectiveness of Sentinel-2 MSI imagery, corrected using the Case-2 Regional Coast Colour (C2RCC) algorithm in SNAP software (Sentinel Application Platform), for estimating chlorophyll-a (Chl-a) and total suspended solids (TSS) in Deran Lake, a karstic lake with minimal anthropogenic pressure within Hutovo Blato Nature Park, Bosnia and Herzegovina. In situ measurements were collected in March 2025 using a YSI EXO2s multiparameter probe at ten monitoring stations under the SMART-Water project. TSS was used as a proxy for total suspended matter (TSM). A regression analysis between satellite-derived and measured values showed a strong correlation for TSS/TSM ($R^2 = 0.76$) and a moderate correlation for Chl-a ($R^2 = 0.61$). Spatial averaging over 5×5-pixel windows improved estimation accuracy, yielding R^2 values of 0.85 for TSS/TSM and 0.69 for Chl-a. Thematics maps of SNAP-derived Chl-a and TSS/TSM distribution was performed using QGIS 3.40. Chl-a concentrations confirmed oligotrophic conditions, while TSS patterns aligned with known hydrodynamic features such as inflow zones and sediment resuspension areas. These findings align with other regional studies demonstrating Sentinel-2's potential for monitoring small and optically complex waterbodies when paired with appropriate atmospheric correction, statistical estimators (e.g., mean), and spatial windowing strategies. This work reinforces the value of remote sensing for cost-effective, high-resolution monitoring of inland waters, improving water resource management across diverse ecosystems.

1. Introduction

Water is one of Earth's most essential natural resources, supporting biodiversity, human health, agriculture, and recreation (Hounslow, 2018). Lakes, in particular, are vital freshwater ecosystems, but their water quality is increasingly threatened by urbanization, agricultural runoff, wastewater discharge, and land use changes (Vinçon-Leite and Casenave, 2019). These pressures contribute to nutrient enrichment, leading to eutrophication and harmful algal blooms, which degrade water quality and aquatic habitats (Binding et al., 2023; Feng et al., 2024; Ma et al., 2025; Wang et al., 2025).

Monitoring water quality is essential for managing and protecting these ecosystems. However, conventional methods, such as manual sampling and laboratory analysis, are often labour-intensive, spatially limited, and unable to provide real-time data (Jan et al., 2021), and in Deran Lake, are often hindered by vegetation cover and water inaccessibility, particularly during summer. In this context, satellite-based remote sensing has emerged as a practical and non-intrusive alternative for large-scale and long-term water quality assessment (Cáceres-Merino et al., 2024; Sent et al., 2021). Among available platforms, Sentinel-2 imagery is particularly valuable due to its high spatial and temporal resolution, making it well-suited for capturing short-term variability in small, optically complex inland waterbodies. Three Sentinel-2 satellites (2A, 2B, and 2C) provide imagery with spatial resolution of 10 to 60 m and temporal resolution of max 5 days (Sent et al., 2021). Combined, in situ multiparameter probes and remote sensing technologies offer scalable, efficient alternatives. Probes like the YSI EXO2s allow for high-resolution, real-time measurement of key indicat-

ors such as turbidity and chlorophyll-a (Chl-a), while satellite platforms such as Sentinel-2 provide broad spatial coverage for monitoring water quality trends over time (Fu et al., 2024; Goblirsch et al., 2023; Yang et al., 2022).

Because water surfaces reflect very little light, applying atmospheric correction is a critical step in remote sensing studies focused on water quality (Kyryliuk and Kratzer, 2019; Radin et al., 2020). One commonly used method is the Case-2 Regional Coast Colour (C2RCC) algorithm, which is particularly effective for monitoring low-turbidity environments, such as marine and clear inland waters (Radin et al., 2020; Šiljeg et al., 2024). Previous research has indicated that C2RCC is the atmospheric correction method that produces the lowest errors and shows the strongest correlation with in situ data (Cáceres-Merino et al., 2024). This atmospheric correction algorithm is integrated into the open-source SNAP software (Sentinel Application Platform), developed by European Space Agency. When applied within SNAP, this method generates various outputs, including absorption coefficients for different water constituents, reflectance values by spectral band, and associated uncertainties (Radin et al., 2020). For this study, the key products of interest include Chl-a concentration (conc_chl, milligrams per cubic meter (mg/m^3) which equals to micrograms per litre ($\mu g/L$)) and total suspended matter (TSM) concentration (conc_tsm, grams per cubic meter (g/m^3) which equals to milligrams per litre (mg/L)) (Kyryliuk and Kratzer, 2019).

Deran Lake in Bosnia and Herzegovina, part of the Hutovo Blato Nature Park, was selected as the study area due to its unique hydrodynamic behaviour, ecological integrity, and suitability for remote sensing validation. Influenced by the Krupa River's occasional reverse flow during high-water periods, the

lake experiences significant shifts in hydrodynamics and nutrient cycling (Public Company Nature Park Hutovo Blato, n.d.). With no prior monitoring and minimal anthropogenic pressure, it offers a pristine environment for studying natural processes. The study area's low density of water lilies in early spring allows easier access for fieldwork, while its proximity to infrastructure and the use of amphibious vehicles support practical research deployment.

This study aims to assess the effectiveness of Sentinel-2 MSI imagery combined with the C2RCC atmospheric correction for monitoring Chl-a and total suspended solids (TSS) in Deran Lake. TSS has increasingly been used interchangeably with TSM in optical modelling due to their strong correlation in non-coastal freshwater systems (Alvado et al., 2021; Saberioon et al., 2020). The aim is to validate the automatic product, including Chl-a and TSM, generated by SNAP using the C2RCC atmospheric correction tool by comparing them with in situ field measurements using the EXO2s probe from March 2025. RMSE is a widely used metric for assessing model accuracy, particularly in regression and remote sensing (Chai and Draxler, 2014). It captures both variance and bias by penalizing larger errors more heavily. However, in small sample studies as this one, RMSE can be skewed by outliers. In such cases, the standard deviation of residuals may provide a more reliable measure of model precision, as it reflects error spread without emphasizing magnitude (Glavačević et al., 2025; Meyer, 2012). The measured and remotely sensed data were compared to obtain the coefficient of determination (R^2), root mean square error (RMSE), standard deviation, and mean absolute percentage error (MAPE) for both Chl-a and TSS/TSM. Such error metrics have been commonly employed in similar studies to validate remote sensing-based retrieval models (Cáceres-Merino et al., 2024; Kyriliuk and Kratzer, 2019; Radin et al., 2020; Sent et al., 2021).

Special emphasis is placed on evaluating how different spatial averaging window sizes, using the mean estimator, affect the accuracy of these estimates. The methodology builds on recent advances in inland water monitoring using satellite data and regionally adapted atmospheric correction algorithms (Jang et al., 2024; Llodrà-Llabrés et al., 2023).

2. Materials and Methods

2.1 Study Area

Deran Lake is located in southern Bosnia and Herzegovina and forms part of the Hutovo Blato Nature Park (Figure 1), a protected wetland system of international ecological importance. The park spans across the municipalities of Čapljina and Stolac, bordering Croatia and forming a significant component of the Neretva River delta ecosystem (Ecoplan, 2014). Deran Lake is one of six interconnected lakes within the park and plays a crucial role in regional biodiversity and water regulation. Its outlet, the Krupa River, exhibits reverse flow behaviour during high-water periods, temporarily bringing water back from the Neretva River and significantly influencing lake hydrodynamics and nutrient cycling (Public Company Nature Park Hutovo Blato, n.d.). Covering an area of approximately 1.4 km² during high water periods and shrinking to 0.3 km² during the dry season, Deran Lake has an average depth of 2 meters and displays strong seasonal variability in both water level and vegetation cover (Public Company Nature Park Hutovo Blato, n.d.). This variability is amplified by the regional karst hydrogeology and influenced by infrastructure such as the Čapljina hydropower

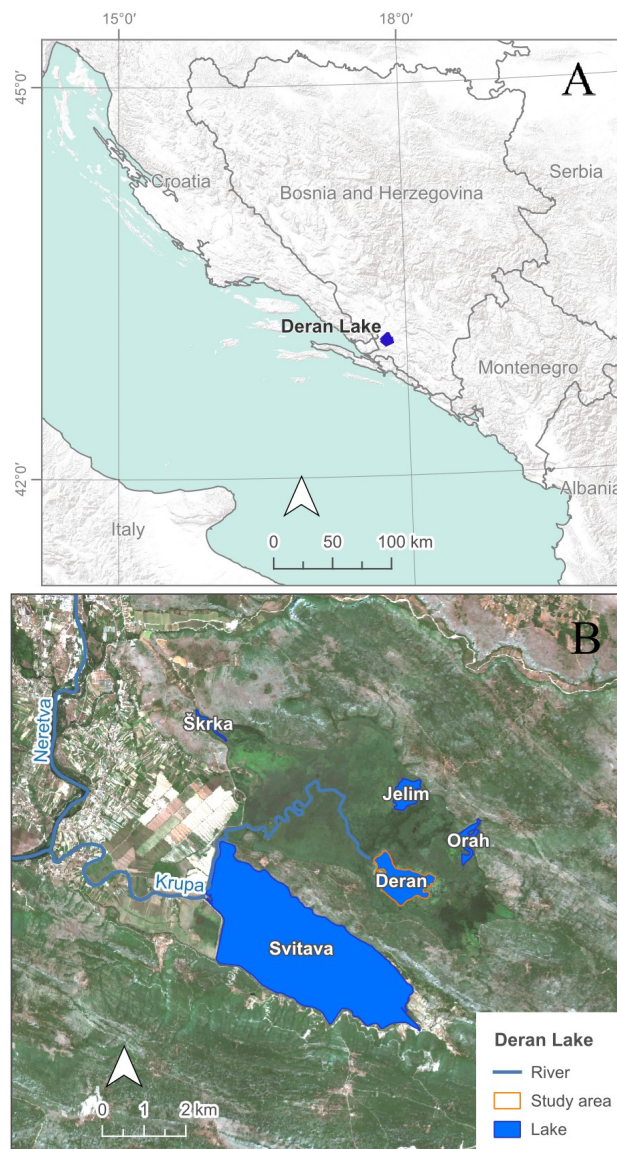


Figure 1. Location of (A) Deran Lake in southeastern Europe and (B) Deran Lake and surrounding waterbodies.

plant, which alters the natural inflow patterns depending on precipitation and losses along the Trebišnjica River (Ecoplan, 2014). Numerous springs, both permanent and intermittent, further support the hydrological complexity of the lake. The study area was selected due to minimal anthropogenic disturbance and unique hydrodynamic features. In summer, the lake becomes heavily covered by water lilies, hindering conventional sampling and satellite-based observations. Therefore, research efforts focused on an accessible time of year when water lily density is relatively low, enabling better conditions for sensor deployment, in situ sampling, and remote sensing validation. The proximity to the Krupa River also allows for the examination of flow reversals and their impact on water quality.

2.2 Study Area Boundary

To accurately delineate the boundary of Deran Lake, the Normalized Difference Water Index (NDWI) was applied using Sentinel-2 satellite imagery. Given the lake's shallow depth and seasonal fluctuations, imagery from August 2024 (low water) and December 2024 (high water) was selected. Cloud-free

Level-2A images were used to ensure reliable data. The NDWI was calculated using Band 3 (green) and Band 8 (near infra-red) in QGIS 3.40 with the formula (McFeeters, 1996):

$$NDWI = (Band3 - Band8) / (Band3 + Band8), \quad (1)$$

The resulting raster outputs were converted into polygon layers. To refine the boundaries, polygons were buffered 15 meters outward and then inward to eliminate edge artifacts. These were further simplified to include only valid water pixels. The final study area was defined based on the December (high water) extent to ensure that the maximum surface area was captured for analysis. Figure 2 illustrates the change in water extent between the two time periods.

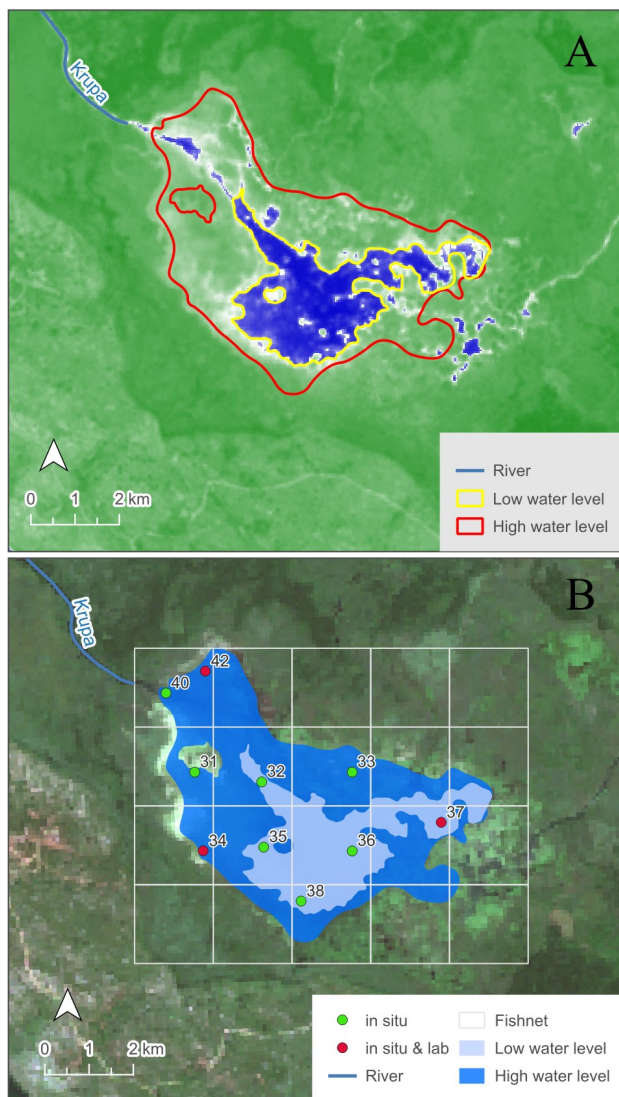


Figure 2. Map of (A) NDWI water levels and (B) monitoring grid.

2.3 In Situ Sampling

As part of this study, a new monitoring grid was developed specifically for Deran Lake to support remote sensing-based analysis. The grid was designed to optimize spatial coverage while accounting for lake's hydrological features. The final monitoring grid for Deran Lake includes ten stations,

strategically distributed across the lake using a 350 m × 350 m fishnet grid (Figure 2B). All stations were used for multi-parameter probe measurements, collecting data on water quality parameters such as turbidity and Chl-a. At three of these stations, additional manual water sampling was conducted to measure TSS and evaluate its relationship with turbidity.

The EPA Method 160.2 procedure for determining TSS in freshwater samples involving a gravimetric analysis was followed. Samples were collected via a hand-grab technique, ensuring minimal disturbance of the water column. At each sampling station, a clean, pre-rinsed 1 L polyethylene bottle was submerged to a depth of approximately 0.2 m to collect the sample. Samples were wrapped in aluminium foil to prevent any microbiological activity that could alter the concentration of suspended solids until the analysis. Samples were immediately stored at 4°C in a portable fridge and transported to the laboratory within 3 hours. In the laboratory, samples were thoroughly mixed in order to evenly distribute particles in the bottle and ensure homogeneity. Furthermore, they were filtered through pre-weighed Glass microfiber filters (LGG Labware; pore size 1.6 µm; filter diameter Ø 47 mm) using a filtration system (MF31, Rocker Scientific) connected to a vacuum pump (Büchi® V-500). The funnel walls were thoroughly rinsed with Milli-Q® water to transfer all remaining particles to the filters. Filtered volume was marked down for each sample. The filters were then dried at 105°C until constant weight (weight change <0.5 mg), cooled in a clean environment, and reweighed to determine the TSS concentration, expressed as grams per cubic meter (g/m^3) which equals to milligrams per litre (mg/L). The TSS concentration was calculated using the following equation:

$$TSS(g/m^3) = ((W2 - W1) * 1000) / V, \quad (2)$$

where $W2$ = final weight of filter + solids (mg)
 $W1$ = initial filter weight (mg)
 V = sample volume (mL)

To support satellite-based modelling and validate empirical relationships, in situ measurement and sample collection was conducted on March 21, 2025, during high water levels to minimize interference from aquatic vegetation.

2.4 Regression Modelling of TSS and Turbidity

To assess the predictive relationship between turbidity and TSS, a simple linear regression model was developed using measured values from three water samples collected during the March 2025 field campaign. Turbidity values, expressed in Formazin Nephelometric Units (FNU), were used as the independent variable, while laboratory-derived TSS values (g/m^3) served as the dependent variable. The regression equation was derived from the least squares method and took the form:

$$TSS = 6.8407 * Turbidity - 4.6453, \quad (3)$$

where TSS = measured TSS (from lab)
 $turbidity$ = measured turbidity (from EXO2s)

The coefficient of determination (R^2) was calculated to evaluate the goodness-of-fit. All calculations were performed in Microsoft Excel. To evaluate model performance, predicted TSS values were compared against measured values, and the percentage prediction error was calculated for each sample. Despite the small sample size, results suggest a strong linear relationship and the practical potential for using turbidity measurements as a real-time indicator of TSS in shallow karstic lake

environments. TSS was treated as a proxy for TSM, due to its close correlation in inland freshwater systems (Saberioon et al., 2020).

2.5 Satellite Data and Atmospheric Correction

Sentinel-2 Level-1C imagery from March 19, 2025, was used for remote sensing analysis. The image was atmospherically corrected using the C2RCC algorithm within the Sentinel Application Platform (SNAP), developed by the European Space Agency. This algorithm applies neural network inversion techniques to convert top-of-atmosphere (TOA) reflectance into water-leaving reflectance (NASA, 2010), which is critical for analysing optically complex inland waters such as Deran Lake. The C2RCC algorithm has been widely validated in various European inland water systems (Gurlin et al., 2011; Odermatt et al., 2012). All bands were resampled to a uniform spatial resolution of 10 meters to ensure consistency across calculations. Key environmental parameters used in C2RCC are listed in Table 1.

To calculate the coefficients *chl_fac*, *chl_exp* (for Chl-a) and *tsm_fac*, *tsm_exp* (for TSM) from measured field data and C2RCC-derived inherent optical properties, a regression analysis was performed, specifically log-log linearization of the power-law relationship (C2RCC, n.d.). The C2RCC-derived empirical model for Chl-a is (C2RCC, n.d.):

$$CHL = chl_fac * (iop_apig)^{chl_exp}, \quad (4)$$

where *CHL* = measured Chl-a (from EXO2s)
iop_apig = phytoplankton pigment absorption at 443 nm
chl_fac, *chl_exp* = model coefficients

$$TSS = tss_fac * (iop_btot)^{tss_exp}, \quad (5)$$

where *TSS* = predicted TSS (from lab)
iop_btot = total particulate backscattering
tss_fac, *tss_exp* = model coefficients

Parameter	Value	Unit	Source
Salinity	0.21	PSU	in situ
Temperature	8.94	°C	C3S (2024)
Ozone	347.37	DU	Sentinel 5P imagery
Air Pressure	1031.77	hPa	C3S (2024)
Elevation	1.48	m	Ecoplan (2014)
TSM factor	5.26	-	C2RCC (n.d.)
TSM exponent	-1.31	-	C2RCC (n.d.)
Chl-a factor	0.15	-	C2RCC (n.d.)
Chl-a exponent	-0.74	-	C2RCC (n.d.)

Table 1. Key parameters used in C2RCC.

2.6 Spatial Averaging and Estimation Approach

To investigate the influence of spatial resolution and averaging strategies on Chl-a and TSS/TSM estimation, three spatial window sizes were analysed: 1x1 (no averaging), 3x3, and 5x5 pixels. For each window, the mean estimator was applied, calculating the mean reflectance value of pixels that met specific quality criteria, excluding no-data values. Mean estimator was chosen due to its relevance in practical monitoring applications and its frequent use in aquatic remote sensing studies (Dörnhöfer and Oppelt, 2016; Mishra and Mishra, 2012). Despite its tendency to slightly underestimate peak values, mean estimator provides a realistic representation of average lake conditions in small waterbodies across Europe, and recent studies

also support its effectiveness for both Chl-a and TSS/TSM estimation (Cáceres-Merino et al., 2024; Radin et al., 2020). In order to select the pixel window that provides variables closest to in situ data, the measured and remotely sensed data were compared to obtain the R², RMSE, standard deviation, and MAPE for both Chl-a and TSS/TSM. The RMSE was calculated as follows (Sent et al., 2021):

$$RMSE = \sqrt{\frac{\sum_{i=1}^N (sat_i - in\ situ_i)^2}{N}}, \quad (6)$$

and the MAPE was calculated as follows (Sent et al., 2021):

$$MAPE = \frac{1}{N} \sum_{i=1}^N \left| \frac{sat_i - in\ situ_i}{in\ situ_i} \right|, \quad (7)$$

where *sat* = satellite-derived value
in situ = measured value
N = number of measurements
i = measurement index.

3. Results

3.1 Regression Results of Turbidity-TSS Relationship

The linear regression model showed a strong correlation between turbidity and measured TSS, with an R² value of 0.85 (Figure 3), indicating a high degree of explanatory power given the limited sample size (n = 3). Predicted TSS concentrations closely aligned with observed values, yielding absolute percentage errors of 15.88%, 13.97%, and 4.19% for samples 37, 42, and 34, respectively (Table 2). The average error across all samples was 11.34%. Notably, the lowest prediction error occurred in the sample with the lowest turbidity and TSS, suggesting improved model performance under clearer water conditions. These findings support the use of turbidity as a proxy indicator for TSS in optically stable, shallow freshwater systems such as Deran Lake.

ID	37	42	34
W1 (mg)	94.6	92.5	91.8
W2 (mg)	95.5	93.7	92.2
V (mL)	950	1000	990
Turbidity (FNU)	0.84	0.83	0.74
TSS (mg/L)	0.95	1.20	0.40
Predicted TSS (mg/L)	1.10	1.03	0.42
Error (%)	15.88	13.97	4.19

Table 2. Measured vs. predicted TSS with error.

3.2 Validation of SNAP-Derived Chl-a and TSS Using In Situ Data

The field campaign was conducted on March 21, with in situ measurements taken at ten sampling stations. Atmospherically corrected Sentinel-2A imagery from March 19 was used for comparison. For each in situ station, actual values were extracted from a single 1x1 pixel corresponding to the location. Based on the observed Chl-a concentrations (Table 3), the lake can be classified as an oligotrophic, clear-water system, with values ranging from 0.15 to 0.81 mg/m³ (Carlson, 1977).

Figure 4A shows the spatial distribution of Chl-a concentrations, an indicator of phytoplankton biomass and primary pro-

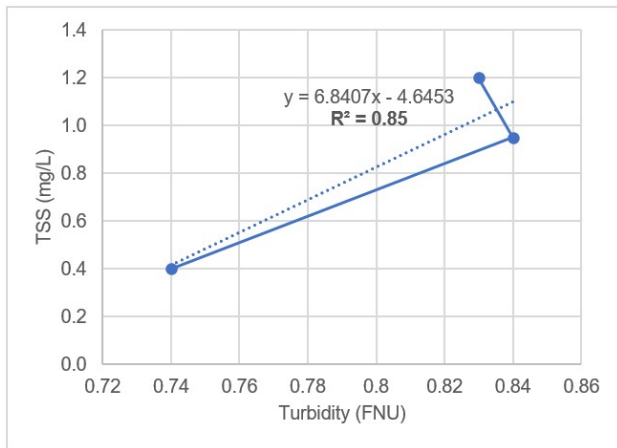


Figure 3. Regression model - TSS (g/m^3) and turbidity (FNU).

ID	In situ		C2RCC	
	Chl-a (mg/m^3)	TSS (g/m^3)	Chl-a (mg/m^3)	TSM (g/m^3)
40	0.30	0.83	0.29	0.96
42	0.25	1.03	0.27	1.12
31	0.39	0.76	0.42	0.79
32	0.31	1.03	0.29	0.80
33	0.27	0.96	0.30	1.13
34	0.28	0.42	0.30	0.50
35	0.29	0.76	0.36	0.67
36	0.25	1.24	0.24	1.40
37	0.37	1.10	0.32	1.21
38	0.28	0.90	0.28	0.78

Table 3. In situ values and estimates derived from Sentinel-2A imagery.

ductivity. Values range from 0.15 to 0.81 mg/m^3 , suggesting generally low Chl-a levels, which is consistent with oligotrophic conditions. Higher concentrations appear in the western and eastern parts of the lake, as well as along some shoreline areas. These localized peaks may be influenced by nutrient inflows, shallow water zones, or aquatic vegetation presence. The spatial pattern indicates moderate heterogeneity, highlighting regions where phytoplankton activity is more pronounced. Figure 4B presents TSM or TSS concentrations, representing all particulate matter suspended in the water column. Values vary from 0.18 to 3.97 g/m^3 , with the highest concentrations observed in the northern and southern parts of the lake. These areas likely receive input from inflowing streams or exhibit more turbulent hydrodynamics, leading to sediment resuspension. Elevated TSM levels can reduce water clarity and influence light penetration, which has implications for aquatic plant and phytoplankton growth.

3.3 Influence of Window Size on Estimation Accuracy

The results presented in the Figure 5 and Table 4 highlight the influence of spatial averaging on the accuracy of remote sensing-derived estimates for Chl-a and TSM. For Chl-a, the R^2 improved slightly from 0.61 using the 1x1 pixel values (no averaging) to 0.69 with a 5x5 averaging window, indicating that moderate spatial smoothing reduces pixel-level noise and improves correlation with in situ data. A similar trend was observed for TSM, where R^2 increased from 0.76 (1x1) to 0.85 (5x5), with the 3x3 configuration already providing a high correlation of 0.82. These improvements in R^2 were accompanied by a consistent decrease in RMSE, from 0.0330 to 0.0288 for

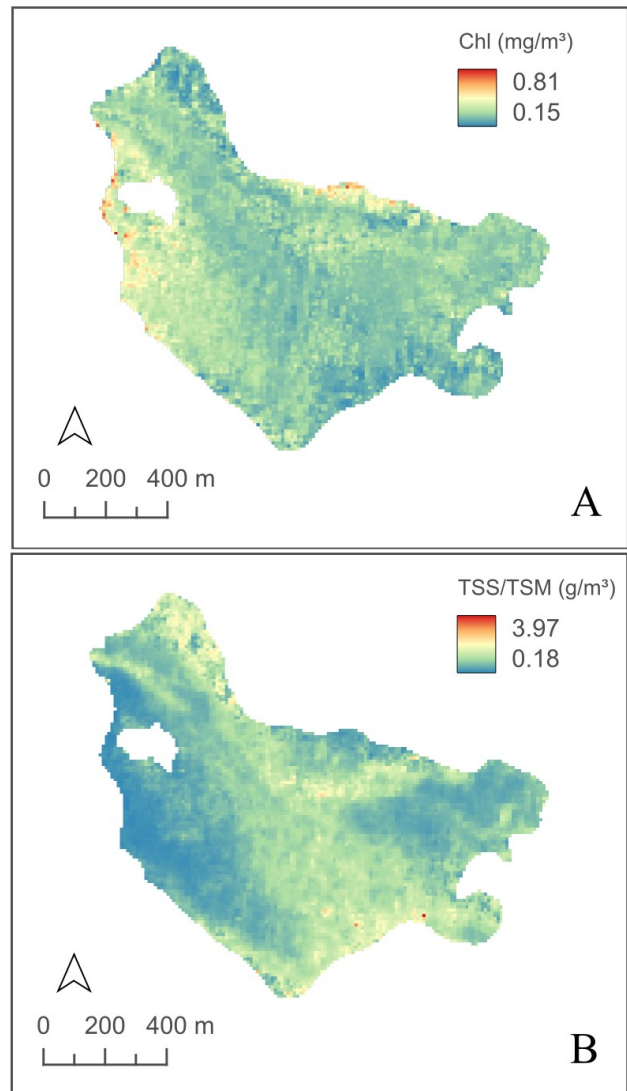


Figure 4. Thematic maps of (A) Chl-a (mg/m^3) and (B) TSS/TSM (g/m^3) for March 19th, 2025 in the Deran Lake.

Chl-a, and from 0.1337 to 0.0962 for TSM. Standard deviation values followed the same trend, decreasing with larger window sizes, and thus suggesting improved stability in the estimates. In this context, it's noteworthy that in the small test sample ($n = 10$), the standard deviation of residuals was nearly twice the RMSE for both parameters. This suggests high variability in model errors despite relatively consistent bias, an effect that is more pronounced with limited data. The reduction in both RMSE and standard deviation with spatial smoothing further supports the reliability of moderate averaging (3x3 or 5x5) in improving model accuracy under small-sample conditions. Additionally, MAPE was lowest with the 5x5 window for Chl-a (7.93%) and TSM (9.53%), further confirming the benefit of spatial averaging. These results indicate that small averaging windows, such as 5x5, effectively balance spatial resolution and noise reduction. For Deran Lake's conditions, the 5x5 configuration appears to be the most effective, likely due to its ability to mitigate edge effects and mixed-pixel contamination without excessively smoothing important local variability.

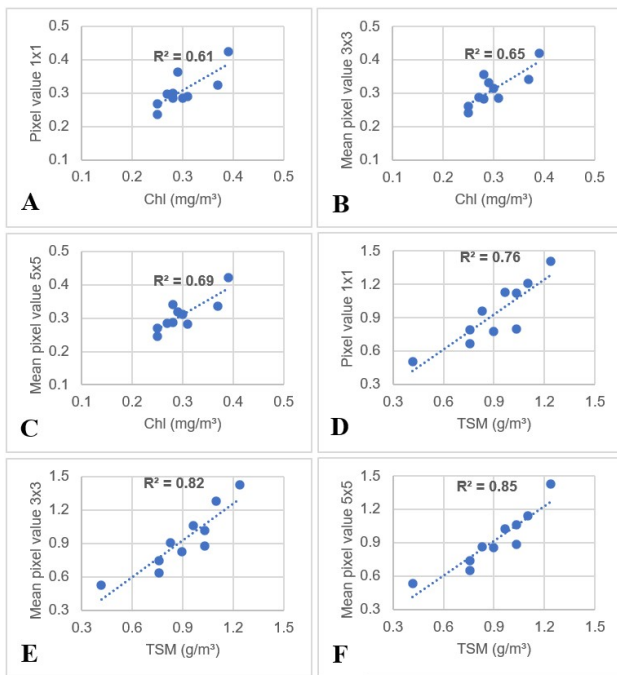


Figure 5. Correlation between in situ Chl-a and TSM measurements and remote sensing pixel values using 1×1, 3×3, and 5×5 spatial windows.

Parameter	Pixel window	RMSE	St.Dev.	R ²	MAPE
Chl-a	1x1	0.0330	0.0476	0.61	8.86
	3x3	0.0326	0.0477	0.65	8.52
	5x5	0.0288	0.0459	0.69	7.93
TSS	1x1	0.1337	0.2417	0.76	13.79
	3x3	0.1174	0.2413	0.82	11.87
	5x5	0.0962	0.2317	0.85	9.53

Table 4. Performance metrics comparing in situ and C2RCC-derived estimates for Chl-a and TSS using different Sentinel-2 pixel window sizes.

4. Discussion

The applicability of remote sensing imagery for water quality monitoring has been extensively supported in the literature. For instance, Batina and Krtalić (2024) provide a comprehensive overview of remote sensing techniques used for monitoring various water quality parameters, emphasizing the significance of atmospheric correction algorithms and validation with in situ measurements. The use of Sentinel-2 MSI imagery, in combination with the C2RCC atmospheric correction algorithms, demonstrated considerable potential for monitoring water quality parameters such as Chl-a and TSS/TSM concentrations in Deran Lake. This aligns with previous research highlighting the suitability of Sentinel-2 data for monitoring inland waterbodies due to its high spatial and spectral resolution (Alvado et al., 2021; Kyrlyuk and Kratzer, 2019; Sent et al., 2021). The findings confirm that spatial context plays a crucial role in reducing noise and improving estimation accuracy. While larger windows reduce noise, they may also smooth out significant features. A 5×5 window size appears to offer the best compromise for Deran Lake, balancing noise reduction with ecological detail retention. This approach has been validated by Cáceres-Merino et al. (2024), who emphasized the need to optimize spatial window sizes when dealing with small or heterogeneous

waterbodies. While RMSE remains useful for assessing overall model performance, standard deviation may better reflect the internal consistency or precision of the model with limited in situ data.

The Krupa River exerts a significant localized influence on the water quality of Deran Lake, particularly near its inflow in the northwestern region. Elevated concentrations of Chl-a in this area suggest increased phytoplankton activity, likely driven by nutrient inputs from the river. Similarly, high levels of TSS/TSM near the river mouth indicate sediment loading from the river. These effects are spatially constrained, with both Chl-a and TSS/TSM levels decreasing toward the central and southeastern parts of the lake. This pattern suggests limited dispersion of riverine inputs, highlighting the Krupa River’s role as a localized but potent driver of biogeochemical variability in Deran Lake.

The increasing reliance on satellite-derived data for monitoring algal blooms and eutrophication trends is further supported by large-scale studies such as Binding et al. (2023) and Ma et al. (2025), who employed long-term remote sensing datasets to monitor bloom dynamics and predict future water quality scenarios. These applications underscore the broader significance of refining satellite algorithms for local-scale studies. Given the close relationship between TSS and TSM in freshwater environments, these results support the integration of TSS retrievals into broader ecosystem assessments (Alvado et al., 2021).

5. Conclusions

This study demonstrates the effectiveness of Sentinel-2 satellite imagery, combined with C2RCC atmospheric correction, for monitoring Chl-a and TSS in Deran Lake. The use of conditional mean estimators and intermediate spatial averaging (e.g., 5×5 pixel windows) was found to enhance predictive accuracy by balancing spatial resolution and noise reduction. Seasonal adaptation of remote sensing methodologies is important, as hydrological conditions significantly influenced model performance. This highlights the need for longer studies to cover all seasons for monitoring strategies in dynamic aquatic environments.

Despite the promising results, remote sensing methods still require rigorous validation against in situ data. This is particularly crucial for periods of low water levels, when in situ sampling becomes challenging. Deran Lake, as a shallow karst-influenced wetland with minimal anthropogenic disturbance, offers a unique and controlled environment for such validation efforts. Furthermore, future work should prioritize increasing the sample size, as a larger dataset improves statistical power, reduces the impact of outliers, and allows both RMSE and standard deviation to provide more stable and meaningful estimates of model performance. This study lays the groundwork for future research and technological deployment under initiatives like the SMART-Water project, highlighting the potential of integrating satellite imagery, remote water quality monitoring, and broader ecological conservation in the Hutovo Blato wetland.

Acknowledgements

We would like to thank Josip Vekić from the Public Company Nature Park Hutovo Blato and the team from the Ruđer Bošković Institute for their valuable support in collecting in situ data. This research was produced as part of the Interreg

SMART-Water (Self-sustainable Multisensor System for Monitoring Water Quality in Inland Waterbodies) project HR-BA-ME00330, funded by the cross-border cooperation Croatia – Bosnia and Herzegovina – Montenegro 2021-2027.

References

- Alvado, B., Sòria-Perpinyà, X., Vicente, E., Delegido, J., Urrego, P., Ruíz-Verdú, A., Soria, J.M., Moreno, J., 2021. Estimating Organic and Inorganic Part of Suspended Solids from Sentinel 2 in Different Inland Waters. *Water* 13, 2453. <https://doi.org/10.3390/w13182453>
- Batina, A., Krtalić, A., 2024. Integrating Remote Sensing Methods for Monitoring Lake Water Quality: A Comprehensive Review. *Hydrol.* 11, 92. <https://doi.org/10.3390/hydrology11070092>.
- Binding, C.E., Zeng, C., Pizzolato, L., Booth, C., Valipour, R., Fong, P., Zastepa, A., Pascoe, T., 2023. Reporting on the status, trends, and drivers of algal blooms on Lake of the Woods using satellite-derived bloom indices (2002–2021). *Journal of Great Lakes Research* 49, 32–43. <https://doi.org/10.1016/j.jglr.2022.12.007>.
- C2RCC, n.d. Neural nets. C2RCC. URL <https://c2rcc.org/neural-nets/> (accessed February 12, 2025).
- C3S, 2024. ERA5 hourly data on single levels from 1940 to present. <https://doi.org/10.24381/CDS.ADBB2D47>.
- Cáceres-Merino, J., Cuartero, A., Torrecilla-Pinero, J.A., 2024. Finding Optimal Spatial Window: The Influence of Size on Remote-Sensing-Based Chl-a Prediction in Small Reservoirs. *IEEE J. Sel. Top. Appl. Earth Observations Remote Sensing* 17, 18769–18783. <https://doi.org/10.1109/JSTARS.2024.3476970>.
- Chai, T., Draxler, R.R., 2014. Root mean square error (RMSE) or mean absolute error (MAE)? – Arguments against avoiding RMSE in the literature. *Geosci. Model Dev.* 7, 1247–1250. <https://doi.org/10.5194/gmd-7-1247-2014>.
- Dörnhöfer, K., Oppelt, N., 2016. Remote sensing for lake research and monitoring – Recent advances. *Ecol. Indic.* 64, 105–122. <https://doi.org/10.1016/j.ecolind.2015.12.009>.
- Ecoplan, 2014. The Hutovo Blato Nature Park Management Plan.
- Feng, L., Wang, Y., Hou, X., Qin, B., Kutser, T., Qu, F., Chen, N., Paerl, H.W., Zheng, C., 2024. Harmful algal blooms in inland waters. *Nat. Rev. Earth Environ.* 5, 631–644. <https://doi.org/10.1038/s43017-024-00578-2>.
- Glavačević, K., Marić, I., Domazetović, F., Šiljeg, A., Pedić, G., Jurjević, L., Panda, L., 2025. Applicability of network real time kinematic (NRTK) approach in soil erosion measurement at different temporal and spatial scales. *Appl. Geomat.* <https://doi.org/10.1007/s12518-025-00612-y>.
- Goblirsch, T., Mayer, T., Penzel, S., Rudolph, M., Borsdorf, H., 2023. In situ water quality monitoring using an optical multiparameter sensor probe. *Sensors* 23, 9545. <https://doi.org/10.3390/s23239545>.
- Gurlin, D., Gitelson, A.A., Moses, W.J., 2011. Remote estimation of chl-a concentration in turbid productive waters — Return to a simple two-band NIR-red model? *Remote Sens. Environ.* 115, 3479–3490. <https://doi.org/10.1016/j.rse.2011.08.011>.
- Hounslow, A.W., 2018. Water Quality Data: Analysis and Interpretation, 1st ed. CRC Press. <https://doi.org/10.1201/9780203734117>
- Jan, F., Min-Allah, N., Düştögör, D., 2021. IoT based smart water quality monitoring: Recent techniques, trends and challenges for domestic applications. *Water* 13, 1729. <https://doi.org/10.3390/w13131729>.
- Jang, W., Kim, J., Kim, J.H., Shin, J.-K., Chon, K., Kang, E.T., Park, Y., Kim, S., 2024. Evaluation of Sentinel-2 Based Chlorophyll-a Estimation in a Small-Scale Reservoir: Assessing Accuracy and Availability. *Remote Sens.* 16, 315. <https://doi.org/10.3390/rs16020315>.
- Kyryliuk, D., Kratzer, S., 2019. Evaluation of Sentinel-3A OLCI Products Derived Using the Case-2 Regional CoastColour Processor over the Baltic Sea. *Sensors* 19, 3609. <https://doi.org/10.3390/s19163609>.
- Llodrà-Llabrés, J., Martínez-López, J., Postma, T., Pérez-Martínez, C., Alcaraz-Segura, D., 2023. Retrieving water chlorophyll-a concentration in inland waters from Sentinel-2 imagery: Review of operability, performance and ways forward. *Int. J. Appl. Earth Obs. Geoinf.* 125, 103605. <https://doi.org/10.1016/j.jag.2023.103605>.
- Ma, J., Duan, H., Chen, C., Cao, Z., Shen, M., Qi, T., Chen, Q., 2025. Projected response of algal blooms in global lakes to future climatic and land use changes: Machine learning approaches. *Water Research* 271, 122889. <https://doi.org/10.1016/j.watres.2024.122889>.
- McFeeters, S.K., 1996. The use of the Normalized Difference Water Index (NDWI) in the delineation of open water features. *Int. J. Remote Sens.* 17, 1425–1432. <https://doi.org/10.1080/01431169608948714>.
- Meyer, P. (2012). Root Mean Square Error Compared to, and Contrasted with, Standard Deviation. *Surveying & Land Information Science*, 72(3), p107.
- Mishra, S., Mishra, D.R., 2012. Normalized difference chlorophyll index: A novel model for remote estimation of chlorophyll-a concentration in turbid productive waters. *Remote Sens. Environ.* 117, 394–406. <https://doi.org/10.1016/j.rse.2011.10.016>.
- NASA, 2010. C2RCC Processor. SeaDAS. URL <https://seadas.gsfc.nasa.gov/help-8.0.0/c2rcc/C2RCCTool.html> (accessed February 12, 2025).
- Odermatt, D., Gitelson, A., Brando, V.E., Schaepman, M., 2012. Review of constituent retrieval in optically deep and complex waters from satellite imagery. *Remote Sens. Environ.* 118, 116–126. <https://doi.org/10.1016/j.rse.2011.11.013>.
- Public Company Nature Park Hutovo Blato, n.d. General information about Hutovo Blato Nature Park (in Bosnian).

URL <https://hutovo-blato.ba/o-parku/> (accessed December 12, 2024).

Radin, C., Sòria-Perpinyà, X., Delegido, J., 2020. Multitemporal water quality study in Sitjar (Castelló, Spain) reservoir using Sentinel-2 images. *Rev. Teledetec.* 117. <https://doi.org/10.4995/raet.2020.13864>.

Saberioon, M., Brom, J., Nedbal, V., Souček, P., Císař, P., 2020. Chlorophyll-a and total suspended solids retrieval and mapping using Sentinel-2A and machine learning for inland waters. *Ecol. Indic.* 113, 106236. <https://doi.org/10.1016/j.ecolind.2020.106236>.

Sent, G., Biguino, B., Favareto, L., Cruz, J., Sá, C., Dogliotti, A.I., Palma, C., Brotas, V., Brito, A.C., 2021. Deriving Water Quality Parameters Using Sentinel-2 Imagery: A Case Study in the Sado Estuary, Portugal. *Remote Sens.* 13, 1043. <https://doi.org/10.3390/rs13051043>.

Šiljeg, A., Cukrov, N., Batina, A., Marić, I., 2024. Spatial-Temporal Assessment of Water Quality Dynamics using Sentinel-2 Satellite Data: Vrana Lake, Croatia. Presented at the 43rd CIESM Congress, Palermo, Italy.

Vinçon-Leite, B., Casenave, C., 2019. Modelling eutrophication in lake ecosystems: A review. *Sci. Total Environ.* 651, 2985–3001. <https://doi.org/10.1016/j.scitotenv.2018.09.320>.

Wang, Y., Zhao, D., Woolway, R.I., Yan, H., Paerl, H.W., Zheng, Y., Zheng, C., Feng, L., 2025. Algal blooms intensify in global large lakes over the past two decades. *Natl. Sci. Rev.* nwaf011. <https://doi.org/10.1093/nsr/nwaf011>.

Yang, H., Kong, J., Hu, H., Du, Y., Gao, M., Chen, F., 2022. A Review of Remote Sensing for Water Quality Retrieval: Progress and Challenges. *Remote Sens.* 14, 1770. <https://doi.org/10.3390/rs14081770>.